Nonlinear analysis of reinforced concrete slabs through the finite element method

Carlos Henrique Hernandorena Viegas[1], Mauro de Vasconcelos Real[2], Eduardo Pagnussat Titello[3]

[1]Engineering School, Federal University of Rio Grande, Brazil
Email: chviegas@furg.br
[2]Engineering School, Federal University of Rio Grande, Brazil
Email: mauroreal@furg.br
[3]Department of Civil Engineering, Engineering School, Federal University of Rio Grande do Sul, Brazil
Email: du.titello@gmail.com

Abstract— One of the significant difficulties in representing the behavior of reinforced concrete structures in mathematical models is the post-cracking non-linearity. And so, reinforced concrete slabs are no exception to the rule. Still, the usual analysis models for this structural element are verified in the elastic regime when the concrete tensile strength is considered. This model is acceptable for the service limit states but not the ultimate limit state. These aspects associated with the great difference in the behavior of concrete when subjected to tension or compression make it necessary to study a nonlinear mathematical model that can represent a reinforced concrete slab subjected to bending, from the beginning of loading until its failure, as accurately as possible. With this, the ANSYS software, from its version 18, made available in its library the Drucker-Prager-Rankine model arranged with two distinct rupture surfaces. A Drucker-Prager criterion for the concrete subjected to compression and a Rankine criterion for concrete in tension. In addition, the software is based on the finite element method, giving the possibility of precise and nonlinear analysis through load and deformation increments, taking into account both elastic and plastic deformations after concrete cracking. Thus, this work aims to present the modeling of reinforced concrete slabs through the Drucker-Prager-Rankine surface, validating the model by comparing it with several experimental tests. The model results were coherent and acceptable, presenting a good approximation of the results of the tests.

I. INTRODUCTION

From the beginning of their loading to failure, the reinforced concrete structures' behavior is considered complex due to their physical and geometric non-linearity. This non-linearity leads to uncertainties regarding structural design [1].

These phenomena are due to relationships such as nonlinear stress-strain curves, the difference between tension and compression behavior, cracking and crushing of concrete, interactions between aggregates and adhesion of steel bars and concrete, and, still, the phenomena of creep and shrinkage of concrete [2, 3].

Despite this, the usual methods for design focus their theories on uncracked concrete, that is, on the elastic regime when the concrete material still resists the tensile stresses. When in a service situation, these analysis theories are seen as efficient. However, when the objective is to evaluate the failure behavior of reinforced concrete elements subjected to bending, examining the after-cracking and plastic behavior is necessary. So fracture, and plastic theories should be included in the analysis [4].

Thus, one of the objectives of this work was to develop a computational model that would simulate the correct behavior of reinforced concrete slabs subjected to bending from the beginning of loading until its failure. As an instrument, the ANSYS software was used, which is based on the Finite Element Method (FEM) and gives the possibility of using volumetric elements with incorporated reinforcement elements, which simulates the steel rebars inside the slab. Furthermore, the program can use the Drucker-Prager-Rankine failure model, which has the characteristic of using two different failure surfaces when the concrete is subjected to tensile or compression stresses.

II.   COMPUTATIONAL MODELING

The ANSYS software was used through its APDL platform, which brings the possibility of developing a text script containing the data entry base and the running of existing models within the libraries of the program itself. It was possible to model the Drucker Prager-Rankine (DP-Rankine) elastoplastic rupture model extended to the HSD (Hardening, Softening, and Dilatation) subroutine. The concrete material is represented by the volumetric finite element SOLID186, which is compatible with plastic behavior materials. The reinforcement finite element REINF265 reproduces the steel. This element can integrate with SOLID186 with perfect adhesion, simulating a reinforced concrete slab in the best possible way.

Finite Elements used

According to the ANSYS Manual [5], the SOLID186 element presents hexahedral, pyramidal, prismatic, or tetrahedral shapes. So the mesh can be adjusted in the best possible way to the model's geometry. Furthermore, it is formed by 20 nodes and three degrees of freedom (translation in the X, Y, and Z axes) in each node, with quadratic interpolation functions. The element is present in Fig. 1.
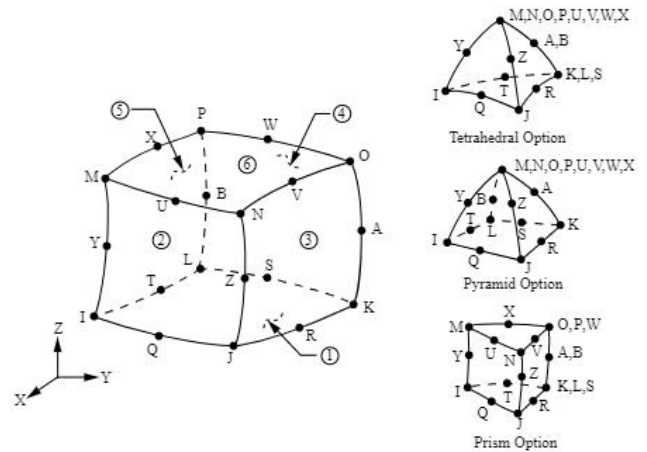

Fig.1: SOLID186 element. Adapted from [5]

The REINF265 element, presented in Fig. 2, shares the same nodes and connectivity as the base element (SOLID186). The element uses the smeared approach. So it is possible to represent equally spaced reinforcing rebars as a surface, generating a significant computational gain in relation to the discrete reinforcement. The main parameters of the element are the reinforcement material, the relative position, the reinforcement cross-section, and the desired spacing for the rebars [5].
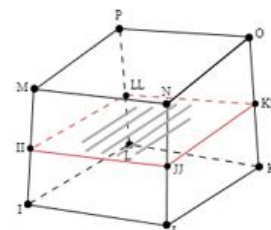

Fig.2: REINF265 element. Adapted from [5]

III.   CONSTITUTIVE MODEL OF MATERIALS

The theories used to simulate two-dimensional surface structures, such as shells and plates, aim to adjust empirical equations to the behavior of the stress-strain law of the element.

Still, it is complicated to establish an accurate description of the performance of the three-dimensional structure until its rupture through the most used elastic models through the concepts of Hook's law alone. Thus, the best possibility to have a result close to reality is to develop an analysis through incremental load and deformation modules using the combined principles of elasticity and plasticity.

In this regard, Chen [6] describes that elastic models should be used in conjunction with failure criteria of the concrete material, where the failure surfaces in the space of principal stresses are used to build an initial and later yield surface based on the theory of plasticity.

Furthermore, Chen [6] proposes that concrete under triaxial compression may present ductile behavior on the yield or rupture surface before reaching the condition of crushing. In this way, a complete plastic model can be adopted, as shown in Fig 3.
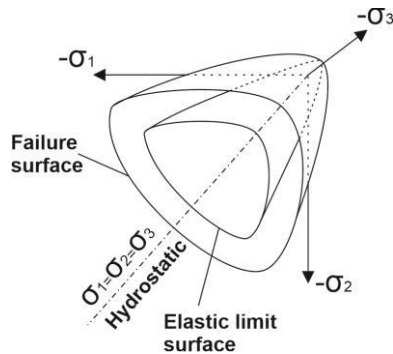

Fig.3: Schematic failure surface of the concrete in three-dimensional stress space. Adapted from [6]

The relationships that must be considered for a perfectly plastic failure model are separated into three parts: before flow (elastic), during plastic flow, and after the fracture (cracking). Thus, the stress invariants' failure criteria are represented through perfectly plastic flow surfaces. For this, a series of numerical models are used.

As a result, plastic failure models use yield models that incorporate a dependence of the yield point stress on the average normal stress (hydrostatic pressure) and the dependence of the invariant on the average maximum shear stress. These models of concrete failure are developed through the strain-hardening plasticity theory. Thus, an increasing loading surface that combines perfect plasticity and strain-hardening after yielding is necessary. This approach is a generalization of the previously mentioned models satisfying the basic principles of continuum mechanics. Thus, a boundary surface for the elastic behavior must be adopted, where the initial flow begins and resembles the rupture surface.

Therefore, the concrete presents failure behavior with plastic deformation in compression and tension. The Young modulus of the elastic region is the same in both cases. In the graph of Fig. 4, it is possible to observe the transition stresses between the elastic medium and the plastic medium where f_c and f_t are given for compression and tension, respectively. At the point of f'_c, the concrete reaches the condition of failure by crushing in compression

for an ultimate strain ε_u; after that, the strength drops to zero. For tensile, the strength and tensile limit are represented by f'_t and ε_t. At the moment of cracking, it is assumed that it occurs in a plane normal to the first principal stress direction. The concrete behavior presents a brittle rupture in the tensioned region. In the plastic regime, unloading behavior in the compressed region is represented by the straight-line BH. The BH line is characterized by following the elastic modulus in parallel to the origin of the diagram.
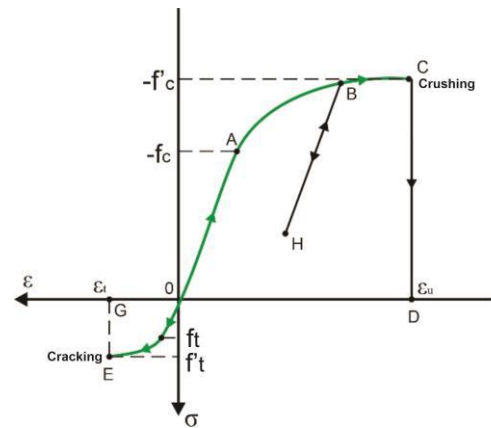

Fig.4: Idealized uniaxial stress-strain curve for concrete. Adapted from [6]

The criteria that define the stress states are characterized by three zones, namely: compression-compression, tensile-compression, and tensile-tensile, as in Fig. 5.
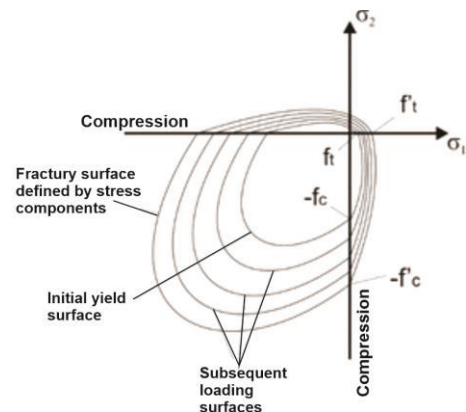

Fig.5: Concrete loading surfaces in the biaxial stress plane for a work hardening plasticity. Adapted from [6]

Drucker-Prager-Rankine

The great challenge in developing a model for simulating reinforced concrete structures is the difference in resistance and deformation behavior in tension and compression. The Drucker-Prager (DP) model is traditionally created to describe the behavior of brittle

failure materials and has been included in the ANSYS library for a considerable time. However, until 2018, the DP offered only one rupture surface. It was not possible to describe the difference in the behavior of concrete when subjected to tensile and compressive stresses, compromising post-cracking results. However, in version 19.2, the software updated the DP to a new Drucker-Prager-Rankine model, containing two distinct rupture surfaces. One for when the element is subjected to compression, implementing the DP, and the other for the element in tension, using the Rankine failure surface. These two failure criteria, together with the possibility of incorporating the reinforcement and using a perfect elastoplastic or bilinear model for steel, made it possible to obtain accurate results compared to experimental tests.

In Fig. 6, the model's input parameters are shown for both tensile and compression stress states. They must be set in the script developed in ADPL language to build the numerical model. The parameters required to use DP-Rankine are:
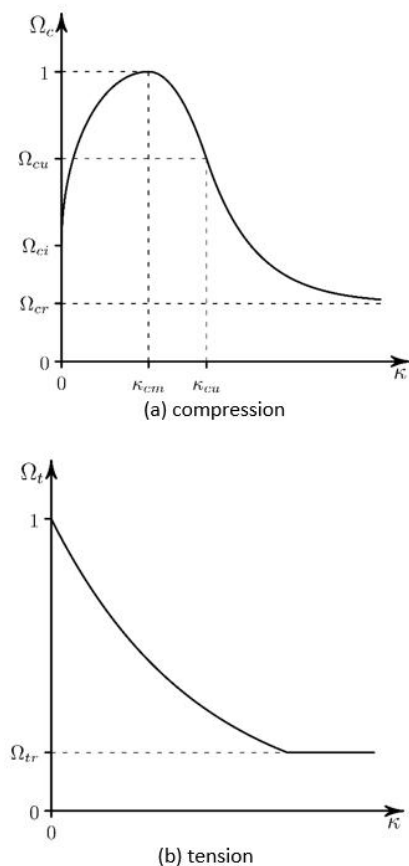

Fig.6: Exponential HSD (hardening, softening, and dilatation) model ANSYS Drucker-Prager Rankine. (a) compression; (b) tension. Adapted from [5]

Dilation factor (δt and δc): the model requests the specification of a dilation factor referring to the surface of the plastic potential. In the present work, the value suggested in the software manual was used, being 0.25 for tension and 1.0 for compression.

Stress factor relative to the beginning of hardening (Ωci), relative stress level (Ωu), residual relative stress level (Ωcr), plastic stress at uniaxial compressive strength (kcm), plastic stress that defines the beginning of exponential softening (kcu) level of residual relative stress in tension (Ωtr), the parameter of plastic deformation when it reaches the level of residual relative stress (ktr).

The ANSYS manual [6] presents the formulations for the behavior of the DP-Rankine rupture surfaces, Fig. 7, represented by the compression-compression, tension-compression, and tension-tension zones as will be demonstrated.

When the value of f_R is below zero, the behavior in tension and tension-compression is admitted in the elastic-linear regime with the tensile strength values remaining constant. However, when f_R reaches zero, the plastic regime begins with the simulation of a crack opening through increments of plastic deformation through an extended model called HSD, responsible for simulating the hardening and softening of concrete during the plastification. ANSYS has four models that can be chosen with different parameters and behaviors. The models are Linear, Exponential, Steel Reinforcement, and Fracture Energy (Fig. 8). The Exponential HSD was used in this work because the behavior characteristics resemble the proposed concrete behavior [5; 7].
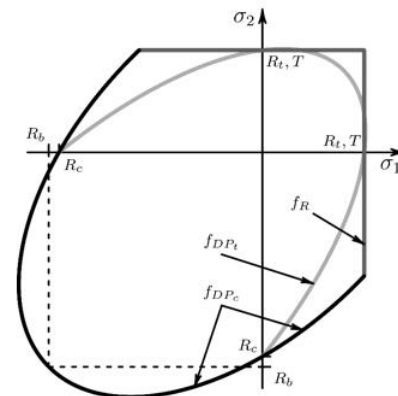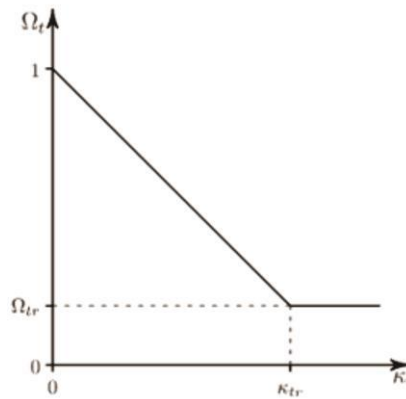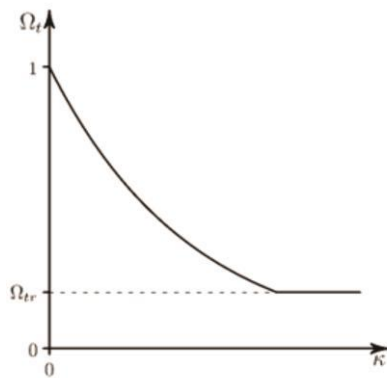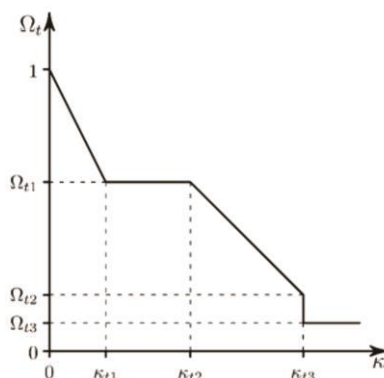

Fig.7: Failure surfaces showing Drucker-Prager and Rankine surfaces. Adapted from [5]
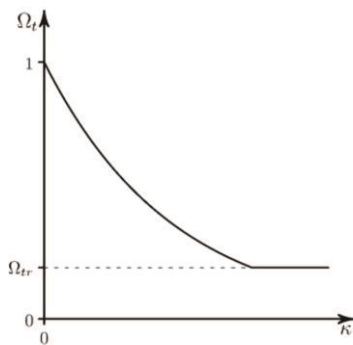
Linear

Exponential

Steel Reinforcement

Fracture Energy

Fig.8: Hardening, Softening, and Dilatation (HSD) Behavior. Adapted from [5]

Drucker Prager compression surface

ANSYS presents the Drucker-Prager compressive loading yield surface formulation given by:

$$f_{DP_c} = \frac{\sigma_e}{\sqrt{3}} + \beta_c \sigma_m - \sigma_{Yc} \Omega_c \qquad (1)$$

$$\sigma_m = \frac{I_1}{3} \qquad (2)$$

$$\sigma_e = \sqrt{3J_2} \qquad (3)$$

where σ_e is given as the von Mises equivalent stress, I_1 is the first stress invariant, J_2 is the second stress invariant, σ_m is the stress average or hydrostatic pressure, and the constants β_c and σ_{Yc} are defined by biaxial compressive strength (R_b) and uniaxial compressive strengths (R_c) strengths

$$\beta_c = \frac{\sqrt{3}(R_b - R_c)}{2(R_b - R_c)} \qquad (4)$$

$$\sigma_{Yc} = \frac{R_b R_c}{\sqrt{3}(2R_b - R_c)} \qquad (5)$$

The variables Ωc and Ωt are hardening and softening functions, both in tension and compression, where they depend on the stress variables σ and hardening "k." From these variables, it is possible to calibrate the model. The flow potential for the Drucker-Praguer tension and tension-compression flow surfaces are given by:

$$Q_{DPc} = \frac{\sigma_e}{\sqrt{3}} + \delta_c \beta_c \sigma_m \qquad (6)$$

where δc is a compression dilation parameter.

Tension and Tension-Compression

William John Macquorn Rankine published, in the year 1876, the Rankine failure criterion, which is known as the maximum tensile stress criterion. The failure occurs when the maximum principal stress reaches the ultimate tensile strength. This strength is obtained through a simple tension test, regardless of the other normal or shear stresses in other planes [6].

The Rankine tensile failure surface becomes fundamental when modeling concrete due to the inefficiency of the Drucker-Prager method in representing the behavior of concrete subjected to tension. Thus, the surface that defines the flow when the principal stress exceeds the tensile strength is given by the equation:

$$f_R = \sigma_m + \frac{2}{3}\sigma_e sen\left(\theta + \frac{2}{3}\pi\right) - T\Omega_t \tag{7}$$

where T is the uniaxial tensile strength.

$$\sigma_m = \frac{\sigma_{11} + \sigma_{22} + \sigma_{33}}{3} \tag{8}$$

$$\sigma_e = \sqrt{3J_e} \tag{9}$$

$$sen(3\theta) = -\frac{\frac{3\sqrt{3}}{2}J_3}{\sqrt{J_2^3}} \tag{10}$$

and, where the stress invariants are given by:

$$J_2 = \frac{1}{6}((\sigma_{11} - \sigma_{22})^2 + (\sigma_{22} - \sigma_{33})^2 + (\sigma_{33} - \sigma_{11})^2) + \sigma_{12}^2 + \sigma_{23}^2 + \sigma_{13}^2 \tag{11}$$

$$J_3 = \det(\sigma - I\sigma_m) \tag{12}$$

Steel Behavior

As a hypothesis, the behavior of the steel in tension and compression is not distinct. The same bilinear model is adopted for both. Since a reinforcement line element represents the steel, only the axial stiffness of the rebar is necessary to be modeled. Two different models can be used for reinforcement steel. The first one, presented in Fig. 9, considers a bilinear behavior for the material. Until the yield stress (f_y), the material is elastic linear with an elastic modulus (E_s). After the yield, the material became plastic with a tangent modulus E_i. The second model, the perfect elastoplastic, presented in Fig. 10, has no hardening after yielding, so $E_i = 0$. Regardless of the models used, the loss of convergence and consequent rupture occurs when the steel strain exceeds the value of 10 ‰.
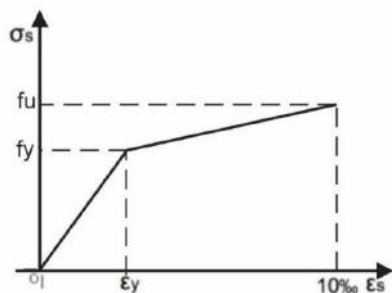

Fig.9: Model stress-strain graph for steel reinforcement with bilinear behavior. Adapted from [5]
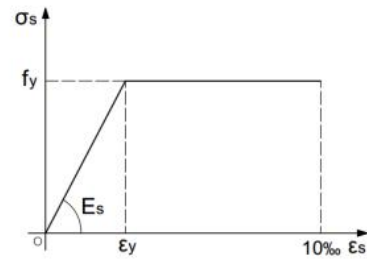

Fig.10: Model stress-strain graph for perfect elastoplastic steel reinforcement. Adapted from [5]

IV.   MODEL VALIDATION

Comparing the results obtained from existing models and with actual data becomes essential to demonstrate the validity of the created model. Thus, the model must be calibrated to lead to parameter adjustments within acceptable ranges. And even the differences between the numerical model results of the experimental test must be minimized for good accuracy. One of the ways to develop this validation is to use data collected from other studies already developed in the laboratory or create new data with the necessary actual conditions.

Data referring to the failure test of sixteen rectangular reinforced concrete slabs, presented in three scientific works, were used for comparison. Seven were supported on four sides among these slabs and nine on two sides.

Model configuration

Two different boundary conditions were used in the modeling of these slabs. Supported on the four sides with vertical constraint, Fig. 11, and supported vertically only on two edges, with the other two free, Fig. 12. The model was developed with a quarter of its original size due to its structural symmetry to obtain an efficiency gain in the computational processing time. Thus, to simulate the complete slab, longitudinal constraints were placed on the internal edges of the slab to ensure no rotation at these points. The mesh used in the study comprises 3x3x3 elements in the three Cartesian dimensions, thus having 27 finite elements for a quarter slab.
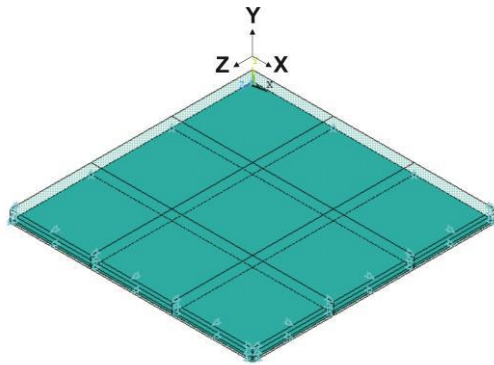
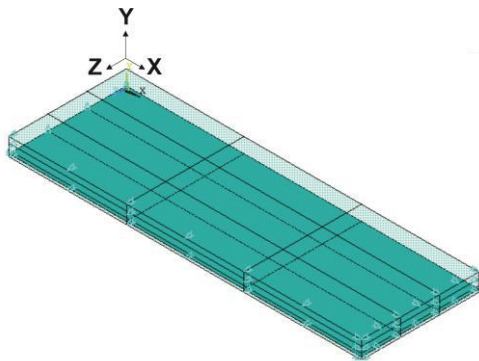*Fig. 11: Slab modeling supported on the 4 borders used in this work.*

Fig. 12: Slab model supported on the two borders used in this work.

Taylor, Maher, and Hayes slabs

In 1966, Taylor, Maher, and Hayes [8], verifying the effectiveness of different configurations of reinforcement distribution in a slab supported on four sides, carried out experimental tests of ten square slabs of reinforced concrete. For this study, it was possible to use three of them called S1, S7, and S9. The characteristic of these slabs is the uniformly spaced distribution of their reinforcements and an orthogonal arrangement of bars.

Pires slabs

Pires [9], in his master's thesis from the Universidade Federal de Minas Gerais, uses the failure data of six single-direction reinforced concrete slabs. This work aimed to study the behavior and failure of monolithic slabs of 10cm (Series 1 A and B) and 15cm (Series 3 A and B) in thickness compared to 10cm slabs with a 5cm reinforced concrete cover. (Series 2 A and B). Slabs named Series 1A, 2A, and 3 (A and B) were chosen to be used in the validation of this model.

Bliuc slabs

In the search for a possible reduction in the thickness of the slabs, Bliuc [10] presented data on failures of reinforced concrete slabs subjected to bending using high-strength concrete. The slabs were supported on four sides (BL3, BL4, BH1, and BH4) and two sides (AH1, AH3, AH4, AL1, and AL4). The concretes had compressive strengths of 65.5 MPa, 77.0 MPa, and 91.5 MPa, with steel yield strength varying between 482.2 MPa and 518.0 MPa.

Analysis of results and discussions regarding model validation

Tab. 1 presents the types of supports used, the identification of the slab, the author, the year of publication, and geometric parameters. Tab. 2 shows the materials' parameters, such as the yield strength of steel (fy), average compressive strength of concrete (fc), and positive reinforcement ratio used in each direction. The parameters for each slab are shown in Tab. 3, where the results of the experimental and ANSYS model failure load values are presented.

Table 1: Geometric parameters of experimental models used for validation

		x	z	y
Slab	**Author**	**L(cm)**	**b(cm)**	**h(cm)**
AH1	Bliuc	240.00	100.00	10.00
AH3	Bliuc	240.00	100.00	10.00
AH4	Bliuc	240.00	100.00	10.00
AL1	Bliuc	240.00	100.00	10.00
AL4	Bliuc	240.00	100.00	10.00
BL3	Bliuc	240.00	240.00	10.00
BL4	Bliuc	240.00	240.00	10.00
BH1	Bliuc	240.00	240.00	10.00
BH4	Bliuc	240.00	240.00	10.00
S1	Taylor. Maher e Hayes	183.00	183.00	5.10
S7	Taylor. Maher e Hayes	183.00	183.00	4.40
S9	Taylor. Maher e Hayes	183.00	183.00	7.60
S1A	Pires	170.00	60.00	10.00
S3A	Pires	170.00	60.00	15.00
S2A	Pires	170.00	60.00	15.00
S3B	Pires	170.00	60.00	15.00

Also, Tab. 3 presents a statistical analysis of the rupture results, with the mean, standard deviation, and coefficient of variation of the failure loads. It was possible to reach the dimensionless average of the ratios of the rupture loads equal to 1.0, demonstrating the convergence of results from the numerical model to the experimental ones. A standard deviation of 0.06 and a coefficient of variation of 6.06% was found. In Fig. 13, the results from

experimental tests and numerical models are compared, where the linear relation has R² = 0.995. The proximity of the experimental results with the numerical model is associated with its good calibration and functioning.

Table 2: Material parameters of the experimental models used for validation.

		x	z	
Slab	**fy(kN/cm²)**	**ρ(%)**	**ρ(%)**	**fc (kN/cm²)**
AH1	48.22	1.13	0.36	6.55
AH3	48.22	1.13	0.36	7.70
AH4	51.80	1.13	0.36	9.15
AL1	48.20	0.57	0.36	6.55
AL4	51.80	0.57	0.36	9.15
BL3	48.20	0.57	0.53	7.70
BL4	51.80	0.57	0.53	9.15
BH1	48.20	1.00	0.97	6.55
BH4	51.80	1.00	0.97	9.15
S1	37.60	0.51	0.55	3.50
S7	37.60	0.55	0.80	3.80
S9	37.60	0.21	0.23	3.30
S1A	68.26	0.79	0.10	3.75
S3A	68.26	0.79	0.10	3.75
S2A	68.26	0.79	0.10	3.75
S3B	68.26	0.79	0.10	3.75

Since the model studied here is based on nonlinear analysis, the structural failure does not occur by strain limits, but by the lack of equilibrium between internal forces and external loads, through the finite element method. Usually, the model becomes unstable when the tensile steel reaches the yield stress, or the compressed concrete reaches its ultimate strain. The convergence tolerance adopted in the analysis was 5% of the Euclidean norm for forces and displacements.

Finally, since it is an element subjected to bending, designed to have a ductile behavior, it was checked that the incorporated reinforcement always reaches its yield stress. The reinforcement yielding was verified for each situation, as demonstrated by the example of slab S7 of [8] in Fig. 14.
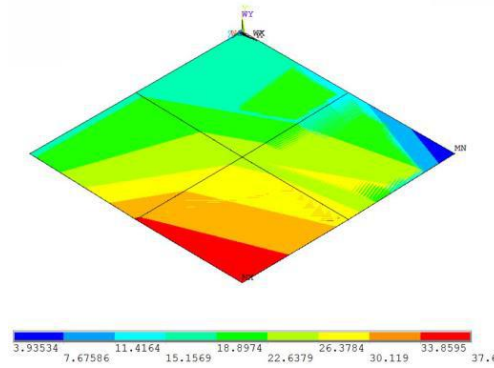

Fig. 14: Tensile stresses (kN/cm²) in steel after the failure of one of the slabs modeled in ANSYS.

Table 3: Results referring to the validation study of the reinforced concrete slab model.

	Breaking load (kN)	
Slab	**Experimental (E)**	**Drucker-Prager-Rankine (DPR)**
AH1	108.70	108.80
AH3	115.90	114.60
AH4	119.00	118.95
AL1	63.32	66.45
AL4	64.45	72.00
BL3	445.00	442.20
BL4	467.00	433.95
BH1	611.00	589.68
BH4	671.00	588.00
S1	90.00	88.88
S7	90.00	88.80
S9	95.86	93.99
S1A	66.40	66.00
S3A	119.00	127.50
S2A	116.57	127.50
S3B	116.36	127.50

Table 4: Material parameters of the experimental models used for validation.

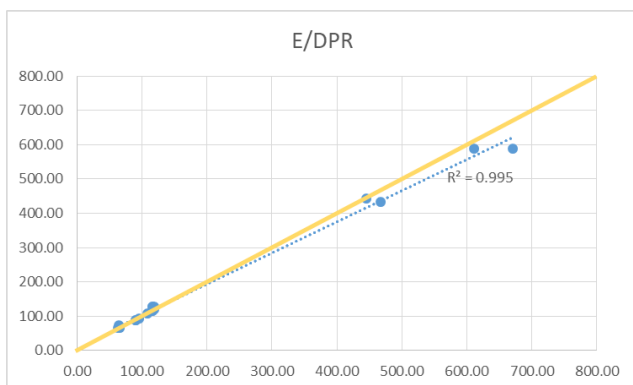| Slab	E/DPR	Average	Standard Deviation	Coefficiente of variation(%)
		Statistic		
AH1	1.00	1.00	0.06	6.37
AH3	1.01			
AH4	1.00			
AL1	0.95			
AL4	0.90			
BL3	1.01			
BL4	1.08			
BH1	1.04			
BH4	1.14			
S1	1.01			
S7	1.01			
S9	1.02			
S1A	1.01			
S3A	0.93			
S2A	0.91			
S3B	0.91			

Fig. 13: Graph with the ratio between the experimental loads and the numerical model DPR and the linear correlation between the rupture loads

V. CONCLUSION

It is possible to conclude from this analysis that reinforced concrete is a heterogeneous material with elastoplastic and nonlinear behavior. This complex behavior generates randomness of results for two elements with the same parameters; as presented in the tests by Pires [9] for slabs S2A and S3A, the result for the rupture will not be the same but similar. In other words, a numerical model that always demonstrates the exact experimental behavior of the test must be questioned, as the properties of concrete vary from one model to another, generating natural randomness. Even so, what was sought with the validation was to demonstrate that the numerical model can obtain good results. In this case, to arrive at the failure load, this work showed that the Drucker-Prager-Rankine model provided by the ANSYS software after calibration could present significant accuracy. It can be considered efficient for analyzing reinforced concrete slabs with failure by bending.

REFERENCES

[1] NASSIM, K.; KHALIL, B.r; BEKADDOUR, B. A.. Nonlinear finite element analysis of reinforced concrete members and punching shear strength of HSC slabs. Matec Web Of Conferences, [s.l.], v. 149, p.02056-02062, 2018. EDP Sciences. http://dx.doi.org/10.1051/matecconf/201814902056

[2] H. G. Kwak and F. C. Filippou, Finite Elements Analysis of Reinforced Concrete Structures Under Monotonic Loads (Report UCB/SEMM-90/14). Berkeley, CA: University of California, 1990

[3] FANNING, P. Nonlinear Models of Reinforced and Post-tensioned Concrete Beams. Electronic Journal of Structural Engineering, Dublin, Ireland, 2001.

[4] CARVALHO, M. L.; SILVA, C. R.; STUCCHI, F. R.. Study on reliability of punching shear of flat slabs without shear reinforcement according to NBR6118. Revista Ibracon de Estruturas e Materiais, [s.l.], v. 10, n. 2, p.276-297, abr. 2017. FapUNIFESP (SciELO). http://dx.doi.org/10.1590/s1983-41952017000200002

[5] ANSYS. Help. 2020. Available in: https://ansyshelp.ansys.com/account/secured?returnurl=/Views/Secured/main_page.html. Acessed in: jun. 2020.

[6] CHEN, Wai-Fah. Plasticity in Reinforced Concrete. New York: McGraw-Hill, 2007

[7] BENINCÁ, M. E. Simulação Numérica de Vigas Alveolares Mistas de Aço e Concreto: Modelo Parametrizado de Elementos Finitos. 2019. 205 f. Master thesis, Porto Alegre, RS, Brazil: Universidade Federal do Rio Grande do Sul

[8] TAYLOR, R.; MAHER, D. R. H.; HAYES, B. Effect of the arrangement of reinforcement on the behavior of reinforced concrete slabs. Magazine of Concrete Research, v. 18, n. 55, p.85-94, 1966.

[9] PIRES, E. F. Comportamento e Desempenho do Reforço à Flexão de Lajes de Concreto Armado através do Aumento da Seção na Região Comprimida. 2003. 100 f. Master thesis, Minas Gerais, MG, Brasil: Universidade Federal de Minas Gerais, Minas Gerais, 2003.

[10] BLIUC, Radu. Particularities of the Structural Behaviour of Reinforced High Strength Concrete Slabs. 2004. 255 f. Doctoral dissertation - Curse of School Of Aerospace, Civil And Mechanical Engineering, Australian Defence Force Academy University Of New South Wales, New South Wales, 2004